Research Paper

Hemispherical Resonator of a Rate-integrating Gyroscope: A Novel Method for Determination of Eigenfrequencies and Eigenforms in Presence of Imperfections

Dmitry Indeitsev[1,2]📷, Pavel Udalov[2]📷, Ivan Popov[2]📷, Alexei Lukin[2]📷

[1] Institute for Problems in Mechanical Engineering of the Russian Academy of Sciences, Saint Petersburg, Russia, Email: Dmitry.Indeitsev@gmail.com

[2] Peter the Great St. Petersburg Polytechnical University, Saint Petersburg, Russia, Email: pp_udalov@mail.ru (P.U.); popov_ia@spbstu.ru (I.P.); lukin_av@spbstu.ru (A.L.)

Abstract. This paper investigates the problem of free vibrations of a hemispherical shell resonator of a rate-integrating gyroscope. A new realization of the approximate Ritz method for determining the frequencies and forms of free vibrations of an elastic hemisphere is proposed. Based on comparison with the results of direct finite-element modeling, it is shown that the proposed approach provides significantly greater accuracy in solving the spectral problem as compared to the solution based on analytical Rayleigh expressions for the forms of pure bending of the hemispherical surface. The importance of considering the potential energy of stretching of the mid-shell surface for the exact determination of frequencies and resonators waveforms for typical geometric parameters is noted. The degree of influence of the introduced refinements into the resonator's mathematical model on the values of frequency splitting associated with gyroscopic forces and mass imperfections is investigated.

Keywords: RIG, Hemispherical resonator, Natural frequency, Ritz method, Rayleigh solution.

1. Introduction

Navigation devices are an indispensable part of modern communication systems, ground, and space systems of orientation of bodies in space. The basis of these devices is the work of sensitive elements - gyroscopes and accelerometers. The resonator of a rate-integrating gyroscope (RIG) vibrates generally in an elliptical eigenform in the operating mode. In the presence of non-zero angular velocity of the platform on which the gyroscope is attached, there is a precession of this standing wave, whose angular velocity is proportional to the angular velocity of the platform (the so-called Bryan effect [1]). The known relationship between angular velocities of the platform rotation and precession (drift) of the excited standing wave can be used to accurately determine the magnitude of the measured component of the angular velocity of the moving object [2, 3]. The sensing element of the RIG can be made in the form of various axisymmetric bodies, which affects the spectrum of possible frequencies and eigenforms [1-5]. The source of vibration excitation in the RIG is a cascade of electrodes, to which periodic voltages are applied [6, 7]. Due to the periodicity of the excitation force in systems of this type, the effect of parametric resonance [1-4], which consists in the formation of swinging zones and damping of oscillations, depending on the geometrical and physical parameters of the system, is observed.

Many research groups and scientists have focused on RIG modelling issues. In [5], a finite-element model of the hemispherical sensitive element of the RIG is investigated. Issues related to the simplifications of the geometry of the investigated object and their influence on the spectrum of natural vibrations of the standing wave are analyzed. In [7-9], the general construction of the natural frequency dependence of a thin hemisphere in the case of predominance of bending deformations over membrane deformations is discussed, and analytical construction of a linear mathematical model of vibrations of the sensitive element of RIG is given. In [8-10], issues related to considering the non-ideality of the material density distribution and the construction of modified expressions for the natural frequencies are discussed.

One of the basic characteristics of practically any sensitive element of the inertial navigation device is the natural frequency of free vibrations [1, 8]. For its determination in the case of simple geometry (beam, disk, ring) there are precise analytical expressions for natural frequencies [6]. In the case of a complex geometry, researchers rely on finite-element calculations of the natural frequencies of the system [3, 5].

A particular issue in the construction of the spectral properties of an axisymmetric body is the derivation of the spectral equation, which is associated with certain hypotheses and assumptions. In the case of considering a hemisphere, researchers use the Rayleigh approximation, which gives accurate results only for thin-walled hemispheres [8, 9]. In practice it is not always possible to achieve thin-walled sensing element due to technical and technological limitations [2, 6]. Then the Rayleigh approximation in advance will give incorrect results compared to the finite-element calculation, which may lead to inoperability of the navigation

device due to non-excitation of the standing wave in it [11]. To avoid this, one should depart from the classical Rayleigh theory [8, 9, 12-15] and consider more accurate theories, such as the Reissner-Mindlin thick-walled shell theories [16-18]. A distinctive feature for studies devoted to the spectral properties of the hemispherical resonator is that, for this case, almost universally only the Rayleigh model of an inextensible thin surface is used, which does not always correctly describe the dynamic properties of the real device [19, 20].

In determining the characteristics of a rate-integrating gyroscope, such as the scale factor [1-6], analytical expressions [1, 4, 6] are applied which include a combination of the resonator eigenforms while considering only bending forms (pure bending forms), that is, thin-walled shells are considered. It follows from this that eigenforms do not depend on geometrical parameters of the resonator (thickness, radius of the midline). Not all resonators are thin-walled and their eigenforms directly depend on the characteristic dimensions of the object. To determine a scale factor in this case an experimental technique may be applied, which gives the same results as analytical expressions [3, 4, 21] in case of thin-walled resonator. This approach is more exact for real resonators, but requires several in-situ experiments, which is not always possible and realizable [2, 5, 6]. Of particular interest is the consideration of the procedure of numerical and semi-analytical derivation of the expressions for the resonator eigenforms and eigenfrequencies, which depend on the physical parameters of the system. Such approach will give modified characteristics at real geometry of a rate-integrating gyroscope and will not require real experiments.

The present paper investigates the problem of free vibrations of a hemispherical shell resonator of a rate-integrating gyroscope. A new realization of the approximate Ritz method for determining the frequencies and forms of free vibrations of an elastic hemisphere is proposed. Based on comparison with the results of direct finite-element modeling, it is shown that the proposed approach provides significantly greater accuracy in solving the spectral problem as compared to the solution based on analytical Rayleigh expressions for the forms of pure bending of the hemispherical surface. The importance of considering the potential energy of stretching of the mid-shell surface for the exact determination of frequencies and resonators waveforms for typical geometric parameters is noted. The degree of influence of the introduced refinements into the resonator's mathematical model on the values of frequency splitting associated with gyroscopic forces and mass imperfections is investigated. The model proposed in the paper allows one to analyze the effect of technologically determined imperfections and gyroscopic forces on the spectral characteristics of a hemispherical resonator with a significantly higher accuracy compared to the conventional approach, while maintaining the advantages of computational compactness.

The paper is organized as follows: In Section 2 the geometric model of a real hemispherical resonator used in production is described. In Section 3 the derivation of the classical Rayleigh equations for determining the eigenspectrum and waveforms of a thin-walled hemispherical shell is discussed. Section 4 describes the numerical Ritz procedure for deriving the eigenforms and frequencies of a hemispherical resonator, considering its physical dimensions. Sections 5, 6 show comparisons of frequency splitting dependencies with account for mass imperfections and gyroscopic forces. Analytical expressions of the frequency splitting for the classical Rayleigh theory and the Ritz approximation expressions are compared. In Section 7 general conclusions about the work are given.

2. Model of the RIG Sensitive Element

The considered sensitive element of RIG (Figs. 1, 2) is a hemispherical quartz resonator, to the pole of which a quartz rod of circular cross-section is attached [3, 5]. At first the possible spectrum of natural frequencies and eigenforms of the resonator was determined. Typical lower forms of vibrations are shown in Fig. 3.

Figure 3(a) corresponds to the case of torsion of the hemispherical shell around the area of its attachment to the rod, which does not make significant movements. Figure 3(b) depicts the natural form of the vibrations of the structure in which the hemispherical shell performs a torsion together with its attachment area to the rod. Figure 3(c) shows the case of horizontal motions of the hemispherical shell as a solid body. Figure 3(d) shows the second bending (elliptic) form of vibrations, which is the working one for the considered gyroscope.
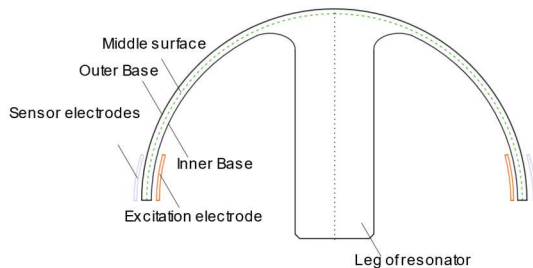

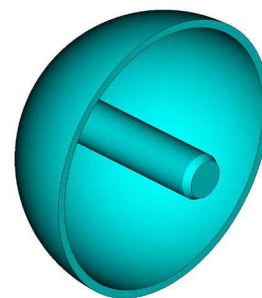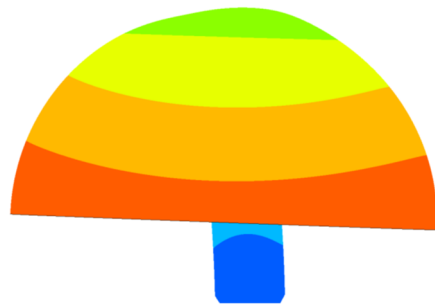Fig. 1. Sensitive element of RIG. Type of assembly.

Fig. 2. Sensitive element of RIG. Isometric view.

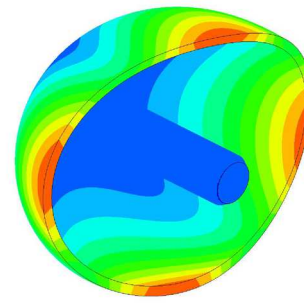(a) Torsional vibrations of the resonator rod

(b) Rolling of the hemisphere

Fig. 3. Eigenforms of oscillations of the sensitive element of the RIG.

(c) Bending of the resonator leg

(d) The second bending (working) form of the resonator vibrations

Fig. 3. Continued.

As the basic (working) form of resonator vibrations the second bending form of free vibrations is chosen [4, 7]. The elliptical form of vibrations of the resonator involves in the deformation only its edge and considering the model with rigid fixation on the pole will be adequate. Thus, the leg of the resonator is discarded from consideration.

3. Spectral Problem for a Hemisphere under the Assumption of Pure Bending

A hemispherical shell of constant thickness h and radius R is considered. Let us represent the components of the vector of displacements of the median surface u, v, w according to the classical theory of vibrations of the rotating shells as [7-9]:

$$u_m = U(m,\theta)[p(t)\cos m\,\varphi + q(t)\sin m\,\varphi],$$

$$v_m = V(m,\theta)[p(t)\sin m\,\varphi - q(t)\cos m\,\varphi], \tag{1}$$

$$w_m = W(m,\theta)[p(t)\cos m\,\varphi + q(t)\sin m\,\varphi],$$

where t – time, $p(t)$, $q(t)$ – modal coordinates, θ, φ – polar and azimuthal angles; $U(m,\theta), V(m,\theta), W(m,\theta)$ – Rayleigh functions determining the natural bending waveforms of an inextensible shell [7-9]:

$$U(m,\theta) = -V(m,\theta) = \sin\theta \tan^m\left(\frac{\theta}{2}\right), \qquad W(m,\theta) = -(m+\cos\theta)\tan^m\left(\frac{\theta}{2}\right). \tag{2}$$

According to the Novozhilov-Goldenweiser theory of thin isotropic shells [12-14], the potential energy Π_b is written as:

$$\Pi_b = \frac{Eh^3R^2}{24(1-\nu^2)}\int_0^{\frac{\pi}{2}}\int_0^{2\pi}[(\kappa_1+\kappa_2)^2 - 2(1-\nu)(\kappa_1\kappa_2 - \kappa_{12}^2)]\sin\theta\,d\theta d\varphi, \tag{3}$$

where $\kappa_1, \kappa_2, \kappa_{12}$ – components of the bending strain tensor [5]:

$$\kappa_1 = \frac{1}{R^2}\left(\frac{dU_m}{d\theta} - \frac{d^2W_m}{d\theta^2}\right)[p(t)\cos m\,\varphi + q(t)\sin m\,\varphi],$$

$$\kappa_2 = \frac{1}{R^2}\left(\cot\theta\,U_m + \frac{m^2}{\sin^2\theta}W_m - \cot\theta\frac{dW_m}{d\theta} - \frac{m}{\sin\theta}V_m\right)[p(t)\cos m\,\varphi + q(t)\sin m\,\varphi], \tag{4}$$

$$\kappa_{12} = \frac{1}{R^2}\left(\frac{m}{\sin\theta}U_m - \cot\theta\,V_m + \frac{m\cot\theta}{\sin\theta}W_m + \frac{dV_m}{d\theta} - \frac{m}{\sin\theta}\frac{dW_m}{d\theta}\right)[-p(t)\sin m\,\varphi + q(t)\sin m\,\varphi].$$

Substituting equation (4) into equation (3), we obtain [5]:

$$\Pi_b = \frac{\pi m^2(m^2-1)^2 Eh^3}{6(1+\nu)R^2}\int_0^{\pi/2}\frac{\tan^{2m}\left(\frac{\theta}{2}\right)}{\sin^3\theta}d\theta\,[p^2(t)+q^2(t)]. \tag{5}$$

The kinetic energy T_s of the hemispherical shell is given by the expression:

$$T_s = \frac{\pi\rho hR^2}{2}\int_0^{\pi/2}[\dot{u}_m^2 + \dot{v}_m^2 + \dot{w}_m^2]\sin\theta\,d\theta, \tag{6}$$

where $(\dot{\ })$ denotes the time derivative of t.

Substituting equations (1) and (2) into equation (6), we obtain:

$$T_s = \frac{\pi\rho hR^2}{2}\int_0^{\pi/2}[U^2(m,\theta) + V^2(m,\theta) + W^2(m,\theta)]\sin\theta\,d\theta[\dot{p}^2(t)+\dot{q}^2(t)]. \tag{7}$$

The Euler-Lagrange equations describing the dynamics of a hemispherical shell have the following form:

$$\frac{d}{dt}\frac{\partial L}{\partial\dot{p}} - \frac{\partial L}{\partial p} = 0, \qquad \frac{d}{dt}\frac{\partial L}{\partial\dot{q}} - \frac{\partial L}{\partial q} = 0, \tag{8}$$

where $L = T_s - \Pi_b$.

Substituting equation (5) and (7) into equation (8), write the system of equations of free vibrations of the hemispherical shell as:

$$\ddot{p} + \lambda_m^2 p = 0, \qquad \ddot{q} + \lambda_m^2 q = 0, \tag{9}$$

where λ_m is the natural frequency of oscillations of a thin hemispherical shell:

$$\lambda_m^2 = \frac{m^2(m^2-1)^2 Eh^2}{3(1+\nu)\rho R^4} \frac{\int_0^{\pi/2} \frac{tan^{2m}\left(\frac{\theta}{2}\right)}{sin^3\theta} d\theta}{\int_0^{\pi/2}[U^2(m,\theta) + V^2(m,\theta) + W^2(m,\theta)] \sin\theta \, d\theta}. \tag{10}$$

To determine the natural frequencies and forms of oscillations, which give a more accurate solution compared to the Rayleigh solution for any relation h/R, the Ritz variational method is used, considering the stretching energy of the mid-surface.

4. Approximate Solution of the Spectral Problem for a Hemispherical Shell Considering Membrane Deformations

Due to the symmetry of the system with respect to the value of φ using the Ritz method [22], the approximate solutions of the $\tilde{u}_m, \tilde{v}_m, \tilde{w}_m$ components of the displacement vector of the shell midline are searched in the form:

$$\tilde{u} = \tilde{U}(\theta)\cos m\varphi\cos\Omega t, \qquad \tilde{v}_m = \tilde{V}(\theta)\sin m\varphi\cos\Omega t, \qquad \tilde{w}_m = \widetilde{W}(\theta)\cos m\varphi\cos\Omega t, \tag{11}$$

where $\Omega, \tilde{U}, \tilde{V}, \widetilde{W}$ are unknown natural frequency and components of the eigenform of oscillations of the hemispherical shell.

To determine the magnitudes $\tilde{U}(\theta), \tilde{V}(\theta), \widetilde{W}(\theta)$ we present them as a set of coordinate functions. For the convergence of the method, the coordinate functions must satisfy the essential boundary conditions of the boundary value problem, that is, the kinematic conditions [22]. We determine the specific form of the approximation series for $U(\theta), V(\theta), W(\theta)$ expanding the Rayleigh functions (2) into a Taylor series:

$$\tilde{U}(\theta) = C_3^U \theta^3 + C_7^U \theta^7 + \cdots, \qquad \tilde{V}(\theta) = C_3^V \theta^3 + C_7^V \theta^7 + \cdots, \qquad \widetilde{W}(\theta) = C_2^W \theta^2 + C_6^W \theta^6 + \cdots \quad. \tag{12}$$

where $C_i^U, C_i^V, C_{i-1}^W, i = 3,7$ are constant values selected by analyzing the Taylor series expansion of the Rayleigh functions. The expansion coefficients are given in Table 1.

Expression (12) notes that considering the stretching energy in the derivation of the equations of the hemisphere eigenspectrum is an additional factor in the dynamics of the resonator. Moreover, the eigenforms taking into account the stretching have the same dependence on the polar angle θ with other weight coefficients C_i^U, C_i^V, C_{i-1}^W. These values are determined from the Hamiltonian variational principle [14]:

$$\delta \int_{t_0}^{t_1} (T_s - \Pi_F) dt = 0, \tag{13}$$

where δ is increment of physical quantity; t_0, t_1 are characteristic boundaries of the time interval of the process under consideration, Π_F is total potential energy, considering both bending (3) and stretching of the shell:

$$\Pi_F = \Pi_b + \Pi_s,$$

$$\Pi_s = \frac{EhR^2}{8(1-\nu^2)} \int_0^{\frac{\pi}{2}} \int_0^{2\pi} \left[e_1^2 + e_2^2 + 2\nu e_1 e_2 + \frac{1-\nu}{2}\omega_{12}^2 \right] \sin\theta \, d\theta d\varphi, \tag{14}$$

$$e_1 = \frac{1}{R}\left(w_m + \frac{\partial u_m}{\partial\theta} \right), \qquad e_2 = \frac{1}{R}\left(w_m + u_m\cot\theta + \frac{1}{\sin\theta}\frac{\partial v_m}{\partial\varphi} \right), \qquad \omega_{12} = \frac{1}{R}\left(-v_m\cot\theta + \frac{1}{\sin\theta}\frac{\partial u_m}{\partial\varphi} + \frac{\partial v_m}{\partial\theta} \right),$$

where e_1, e_2, ω_{12} are components of the tangential strain tensor, Π_s is tensile energy of the middle surface of the resonator [12].

For the harmonic solution of equations (9), it is natural to take as a time interval the period of free oscillations $[t_0, t_1] \to [0, 2\pi/\Omega_n]$. Then the problem for determining the eigenfrequencies and eigenforms is defined as:

$$(A - \Omega_n^2 B)C = 0, \tag{15}$$

where A, B are matrices depending on the structure of the kinetic and potential energies of the system, as well as the coordinate functions C:

$$C = [C_1^U, \ldots, C_M^U, C_1^V, \ldots, C_M^V, C_1^W, \ldots, C_M^W]^T. \tag{16}$$

where M is the number of basis functions. In the case under consideration, the coordinate functions are defined by the expressions (12), T is transpose sign.

Table 1. Asymptotic representation of the natural forms of vibrations of the resonator depending on the thickness h.

h, mm	$\tilde{U}(\theta)$	$U(2,\theta)$	$\tilde{V}(\theta)$	$V(2,\theta)$	$\widetilde{W}(\theta)$	$W(2,\theta)$
0,2	$0{,}33\theta^3 + 0.0018\theta^7$		$0{,}33\theta^3 + 0.0002\theta^7$		$\theta^2 + 0.012\theta^6$	
0,8	$0{,}33\theta^3 + 0.0002\theta^7$		$0{,}32\theta^3 + 0.0014\theta^7$		$\theta^2 + 0.0005\theta^6$	
1	$0{,}33\theta^3 - 0.00039\theta^7$	$\dfrac{\theta^3}{3} + \dfrac{\theta^7}{720}$	$0{,}32\theta^3 + 0.0014\theta^7$	$\dfrac{\theta^3}{3} + \dfrac{\theta^7}{720}$	$\theta^2 - 0.004\theta^6$	$\theta^2 + \dfrac{7\theta^6}{720}$
2	$0{,}325\theta^3 - 0.0025\theta^7$		$0{,}31\theta^3 + 0.0009\theta^7$		$\theta^2 - 0.02\theta^6$	
4	$0{,}323\theta^3 - 0.00038\theta^7$		$0{,}31\theta^3 + 0.0005\theta^7$		$\theta^2 - 0.03\theta^6$	

Table 2. Characteristics of the finite element model.

Element type	SHELL 281
Number of nodes	1520
Number of elements	1444

Table 3. Resonator parameters (fused quartz) [6].

Magnitude/description	Value
Density/ρ	2210 kg m^{-3}
Young's modulus /E	73.3 GPa
Poisson's ratio /ν	0.17

Applying methods of symbolic algebra [23], we obtain expressions for the coefficients C of equation (12). Table 1 shows the numerical values of these coefficients depending on the thickness h of the shell at a fixed value of the radius of the median surface $R = 15\ mm$ in the case equations (2) and (15).

To compare the Rayleigh and Ritz solutions, a numerical experiment was performed in the ANSYS APDL software package [24]. As a finite-element model, a hemispherical shell with a rigid fixation on a circular notch in the pole area of the resonator was considered. The inclusion of the notch in the model under consideration means taking into account the influence of the method of fixing the hemisphere on the spectrum of vibrations of the sensitive element. The image and characteristics of the finite-element model are presented in Fig. 4 and Table 2. The physical properties of the resonator are given in Table 3.

The radius of the median surface $R = 15\ mm$ was fixed and the thickness of the resonator h was gradually changed. Next, the values of natural frequencies of bending vibrations and the results of finite-element analysis are compared. Figure 5 shows the plot of the mesh convergence in the case of calculation of the natural frequency corresponding to the second natural bending form of vibrations (see Fig. 3(d)), for the case $h/R = 0.06$. As a finite element, the 8-node element SHELL281 with 6 degrees of freedom, designed to analyze thin and moderately thick shell structures was chosen [24]. The results of the comparison are presented in Figs. 6 and 7.
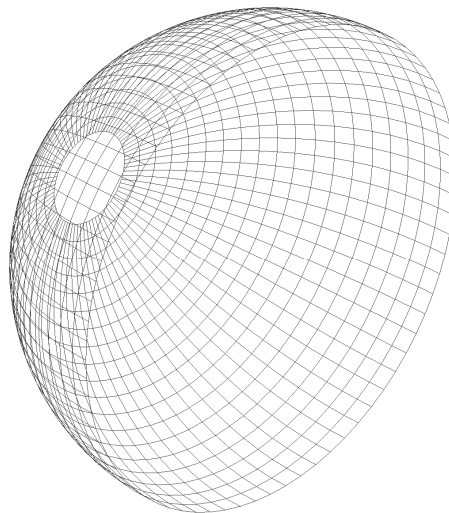

Fig. 4. Finite-element model of the hemispherical resonator; Isometric view.
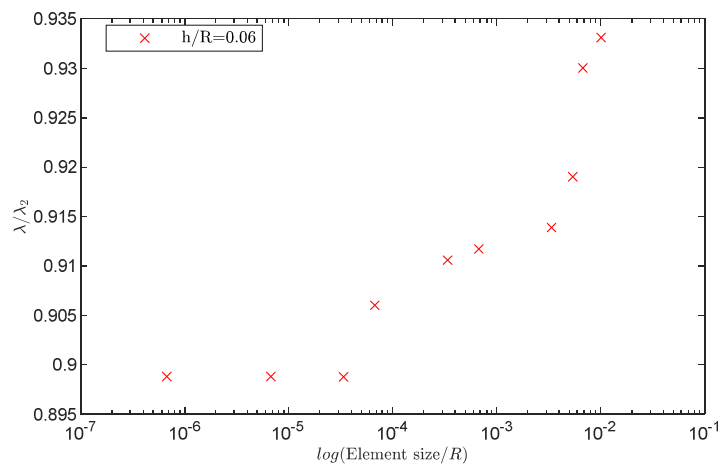

Fig. 5. Diagram of the convergence of the dimensionless frequency $\frac{\lambda}{\lambda_2}$ as a function of the finite-element mesh size.
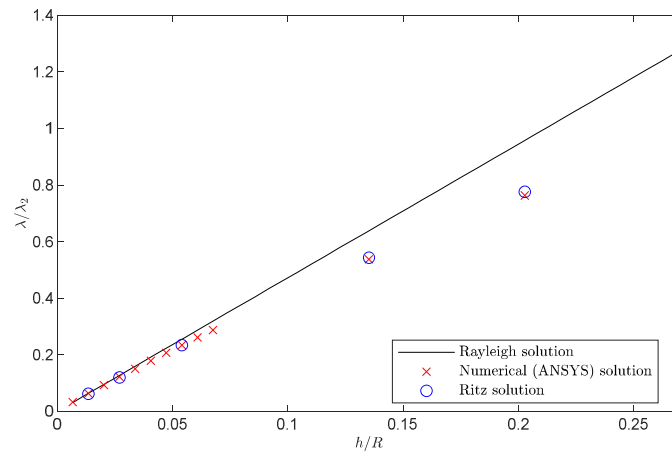
Fig. 6. Dependence of the dimensionless frequency $\frac{\lambda}{\lambda_2}$, on the parameter $\frac{h}{R}$ at $R = 15\ mm$ in the case of the Rayleigh solution [8, 9] (black solid line, Ritz solution (blue circles) and numerical results of ANSYS APDL (red crosses); λ_2 – natural frequency of the resonator, calculated by the Ritz method at h = 2 mm, λ is the second natural frequency of the system depending on the parameter h/R.
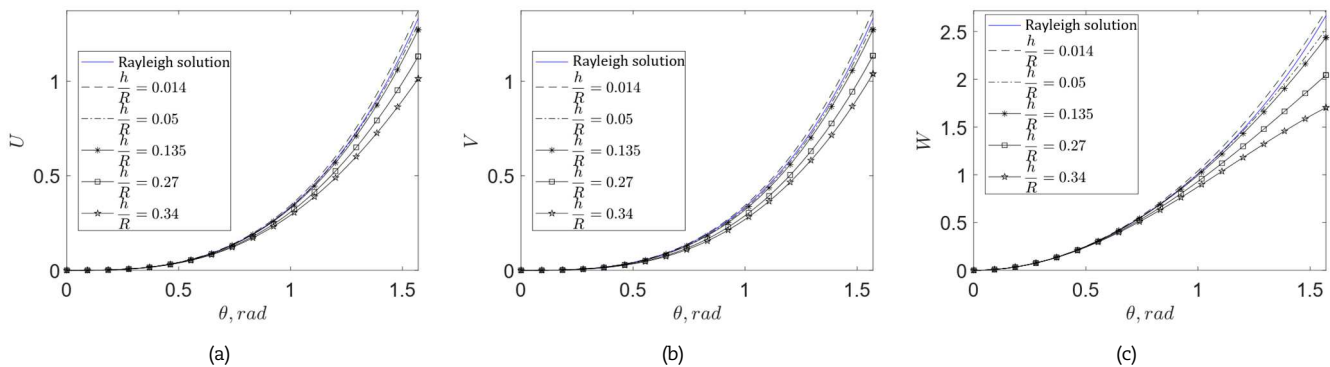

Fig. 7. Dependence of the eigenform component (a) U, (b) V, (c) W at $R = 15\ mm$ in the case of the Rayleigh solution [8,9] (blue line) and the Ritz solution (black lines) ($\frac{h}{R} = 0.014; 0.135; 0.27; 0.34$).

Figure 5 shows that when a certain finite element size is reached, the operating natural frequency of the structure ceases to depend on further reduction of the finite element size. The characteristics of the finite-element model corresponding to a given finite-element size are given in Table 2.

Figure 6 shows that the solution (10) for the natural frequencies of vibrations of the hemisphere is a linear function of the thickness of the shell and gives a close solution in the case of small thicknesses $(h/R \leq 1/5)$ in comparison with the numerical experiment. The approximate Ritz solution (16) has a similar dependence of the natural frequency λ_2 on the thickness h as the numerical experiment. For sufficiently thick shells $(h/R \geq 1/5)$ the Ritz solution takes higher frequency values compared to the numerical values. At $h/R = 1/5$ the difference between the frequencies is 1.6%.

Figure 7 shows the dependences of the eigenforms $U(\theta)$, $V(\theta)$, $W(\theta)$ on the polar angle θ. In the case of Rayleigh expressions [8, 9] the eigenforms do not depend on the resonator thickness, and in the case of the Ritz solution (16) it can be seen that as the resonator thickness increases the functions U, V, W take on different values in comparison to the Rayleigh solution.

Thus, the use of the variational Ritz method allowed us to increase the degree of coincidence of natural frequencies with experimental ones. It is shown that substitution of basis functions (12) obtained from the theory of thin-walled shells into the Ritz method (16) makes it possible to approach the eigenspectrum of a thick-walled shell (that is, a shell for which the tensile energy becomes essential) with an accuracy of 2% at $h/R = 1/5$.

5. Frequency Splitting in the Case of Mass Imperfections of the Resonator

At the stage of development of any navigation device it is necessary to perform many technological operations to determine its properties (level of systematic errors, sensitivity to external influences, natural frequency, etc.). Special attention is paid to studying the effect of splitting of natural frequencies of the sensitive element in the presence of physical or geometric defects [7]. Further, a common defect of non-uniformity of material density distribution of sensitive element RIG is considered. Let us assume that the material density ρ depends only on the angle φ:

$$\rho(\varphi) = \rho_0 + \varepsilon\rho_1(\varphi), \tag{17}$$

where ρ_0 is the density of "ideal" resonator without defects, $\rho_1(\varphi)$ is some distribution of the defect density, ε is a small parameter indicating the smallness of the defect.

Due to the symmetry of the system, the properties of the resonator are periodic with respect to the angle φ, which leads to the following condition for the density:

$$\rho(\varphi) = \rho(\varphi + 2\pi), \tag{18}$$

where it follows that the function $\rho_1(\varphi)$ is periodic. From these considerations, we decompose the function $\rho_1(\varphi)$ into a Fourier series [7]:

$$\rho(\varphi) = \rho_0 + \varepsilon \sum_{j=1}^{\infty} (\rho_{jc} \cos j\varphi + \rho_{js} \sin j\varphi), \tag{19}$$

where ρ_{jc}, ρ_{js} are the coefficients of density decomposition in the Fourier series of the j-th harmonic.

Substituting equation (19) into equation (7), we obtain a modified expression for the kinetic energy T_s^ε:

$$T_s^\varepsilon = \frac{\pi \rho_0 h R^2 I_1}{2} [\dot{p}^2(t) + \dot{q}^2(t)] + \frac{\varepsilon \pi h R^2 I_2}{4} [\rho_{2mc}[\dot{p}^2(t) - \dot{q}^2(t)] + 2\rho_{2ms} \dot{p}(t)\dot{q}(t)], \tag{20}$$

where

$$I_1 = \int_0^{\pi/2} [U^2(m,\theta) + V^2(m,\theta) + W^2(m,\theta)] \sin\theta \, d\theta, \qquad I_2 = \int_0^{\pi/2} [U^2(m,\theta) - V^2(m,\theta) + W^2(m,\theta)] \sin\theta \, d\theta. \tag{21}$$

From equation (21), only harmonics with the doubling the number of harmonic variability by φ of the resonator contribute to the resonator dynamics. To analyze the dependence of the magnitude of the frequency splitting on the defect amplitudes, let us consider only the case of a pure bending of hemisphere. Let's substitute expressions (5) and (21) into expression (8) and obtain the equations of resonator dynamics at considering the mass defect:

$$\left(1 + \frac{\varepsilon \rho_{2mc}}{2\rho_0}\right) \ddot{p} + \lambda_m^2 p + \frac{\varepsilon \rho_{2ms}}{2\rho_0} \frac{I_2}{I_1} \ddot{q} = 0,$$

$$\left(1 - \frac{\varepsilon \rho_{2mc}}{2\rho_0}\right) \ddot{q} + \lambda_m^2 q + \frac{\varepsilon \rho_{2ms}}{2\rho_0} \frac{I_2}{I_1} \ddot{p} = 0. \tag{22}$$

To solve system (22), it takes in form:

$$p = p_c e^{i\lambda t}, \qquad q = q_c e^{i\lambda t}, \tag{23}$$

where λ is the natural frequency of system (22), $i^2 = -1$, p_c, q_c are constants.

The solution of the system (22) with (23) concerning the magnitude of the defect $(\rho_{2ms}^2 + \rho_{2mc}^2)/\rho_0^2$ is written as follows:

$$\frac{\varepsilon^2(\rho_{2ms}^2 + \rho_{2mc}^2)}{\rho_0^2} = 4 \left(\frac{I_1}{I_2}\right)^2 \left(\frac{\lambda_m}{\lambda}\right)^2 \left(\left(\frac{\lambda}{\lambda_m}\right)^2 - 1\right). \tag{24}$$

Equation (24) shows the dependence of the parameter value $(\rho_{2ms}^2 + \rho_{2mc}^2)/\rho_0^2$ denoting the ratio of the defect density amplitude to the ideal resonator density, on the natural frequency λ.

The application of the modified eigenforms shows a qualitative change in the dependence of the resonator frequency on the defect size. When the potential stretching energy is considered in formulas (14) and (24), the values depending on the frequency λ and the resonator eigenforms (parameters I_1, I_2) are changed. By carrying out the procedure described in item 4, the system for determining the magnitude of the defect depending on the natural frequency is similar to system (22), from which we obtain the expression for determining the magnitude of the defect by the value of the resonator frequency splitting.

Figures 8 and 9 below shows the dependences of the natural frequency λ on the defect parameter $(\rho_{2ms}^2 + \rho_{2mc}^2)/\rho_0^2$ in the case of the Rayleigh solution (2) and the solution (15) at different values of the parameter h/R.
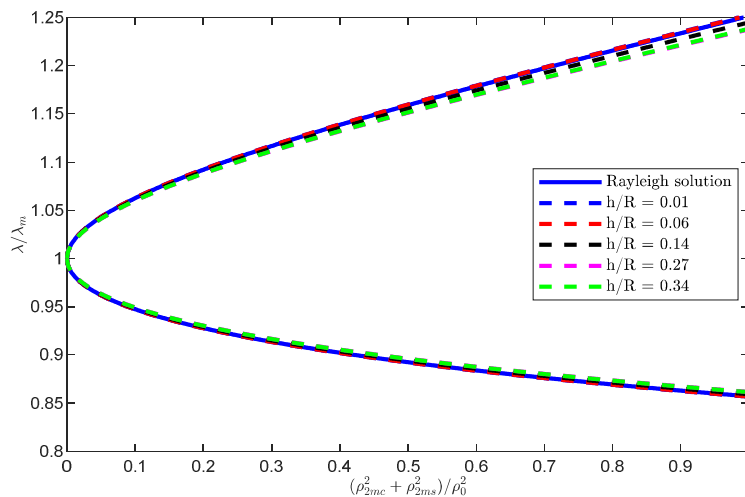

Fig. 8. Dependence of the defect magnitude on the natural frequency of the resonator in the case of the Rayleigh solution (blue solid line) and the solution when considering the potential energy of stretching (dashed lines) at $\varepsilon = 1$; ($h/R = 0.01, 0.06, 0.14, 0.27, 0.34$).
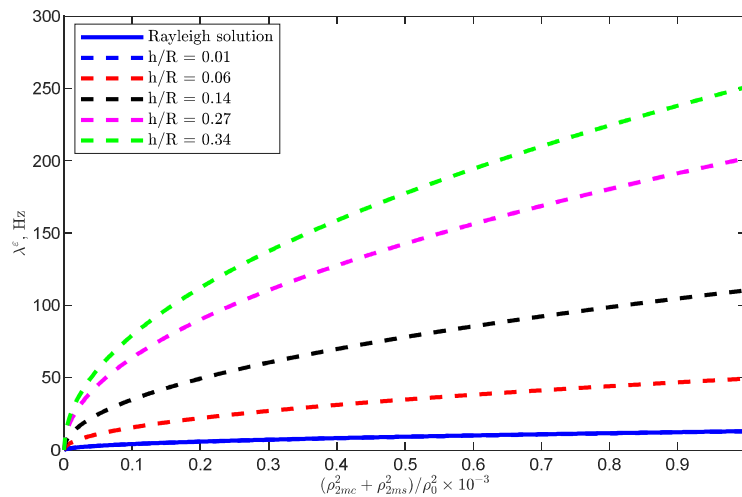
Fig. 9. Dependence of the magnitude of the splitting of the natural frequency λ^ε of the resonator in the case of mass imperfections; $(h/R = 0.01, 0.06, 0.14, 0.27, 0.34)$.

Figures 8 and 9 show that accounting the mass imperfection changes the resonator's natural vibration spectrum. Moreover, when the mass imperfection parameter increases, the magnitude of the splitting of the natural frequencies also increases. It can be seen that taking into account the eigenforms obtained using the Ritz method obtains larger values of the frequency splitting magnitude as compared to the Rayleigh eigenforms. Further, the problem of the effect of splitting of natural frequencies of the resonator at its rotational motion relative to the symmetry axis of the system is considered.

6. Investigation of Gyroscopic Splitting of the Resonator

In the operating mode of RIG operation, the hemispherical shell is subjected to angular motion with angular velocity Ω. Due to angular motion in the system arise gyroscopic and centripetal forces, causing the effect of frequency splitting [25]. Assume that the pseudovector $\boldsymbol{\Omega}$ is directed along the symmetry axis of the resonator, $|\boldsymbol{\Omega}| = \Omega$.

According to Euler's law, the vector of absolute velocity $\boldsymbol{V}$ of an arbitrary point of the resonator is written as follows:

$$\boldsymbol{V} = \dot{\boldsymbol{u}} + \boldsymbol{\Omega} \times (\boldsymbol{r} + \boldsymbol{u}), \tag{25}$$

where $\boldsymbol{u}$ is elastic displacement vector of the resonator midpoint, $\boldsymbol{r}$ is radius vector of the shell point in the reference configuration (undeformed), $|\boldsymbol{r}| = R$, $\times$ is vector product notation. In the projection on the spherical coordinate system equation (25) is rewritten as follows [26]:

$$\boldsymbol{\Omega} = (-\Omega \sin \theta \ \ 0 \ \ \Omega \cos \theta)^T \qquad \boldsymbol{r} = (0 \ 0 \ R)^T,$$

$$\boldsymbol{V} = \begin{pmatrix} \dot{u}_m - \Omega v_m \cos \theta \\ \dot{v}_m + \Omega[(R + w_m) \sin \theta + u_m \cos \theta] \\ \dot{w}_m - \Omega v_m \sin \theta \end{pmatrix}, \tag{26}$$

Considering expression (26), the kinetic energy T_s^Ω of the resonator is:

$$T_s^\Omega = \frac{\rho h R^2}{2} \int_0^{\pi/2} \boldsymbol{V^2} \sin \theta \, d\theta = T_s + \pi \rho h R^2 \Omega \int_0^{\pi/2} [\dot{v}_m((R + w_m) \sin \theta + u_m \cos \theta) - \dot{u}_m v_m \cos \theta - \dot{w}_m v_m \sin \theta] \sin \theta \, d\theta +$$

$$+ \frac{\pi \rho h R^2 \Omega^2}{2} \int_0^{\pi/2} \left[v_m^2 + \left((R + w_m) \sin \theta + u_m \cos \theta \right)^2 \right] \sin \theta \, d\theta. \tag{27}$$

Substituting expressions (1) and (7) into equation (27) and integrating over the angle $\varphi \in [0, 2\pi]$, we obtain:

$$T_s^\Omega = \frac{\pi \rho h R^2 I_1}{2} [\dot{p}^2(t) + \dot{q}^2(t)] - 2\pi \rho h R^2 \Omega I_3 \ [\dot{p}(t) q(t) - p(t) \dot{q}(t)] + \frac{\pi \rho h R^2 \Omega^2 I_4}{2} [p^2(t) + q^2(t)], \tag{28}$$

where $I_3 = \int_0^{\pi/2} [U(m, \theta) \cos \theta + W(m, \theta) \sin \theta] V(m, \theta) \ sin \theta \, d\theta$, $I_4 = \int_0^{\pi/2} \ [(U(m, \theta) \cos \theta \ + \ W(m, \theta) \sin \theta)^2 \ + \ V^2(m, \theta)] \sin \theta \, d\theta$.

Substituting expressions (5) and (28) into expression (8), we obtain:

$$\ddot{p} + \left(\lambda_m^2 - \frac{I_4}{I_1} \Omega^2 \right) p - \frac{4 I_3}{I_1} \Omega \dot{q} = 0, \tag{29}$$

To solve system (29), we take the form:

$$p = p_c e^{i\lambda^\Omega t}, \qquad q = q_c e^{i\lambda^\Omega t}, \tag{30}$$

where λ^Ω is the natural frequency of system (29), p_c, q_c are constants.
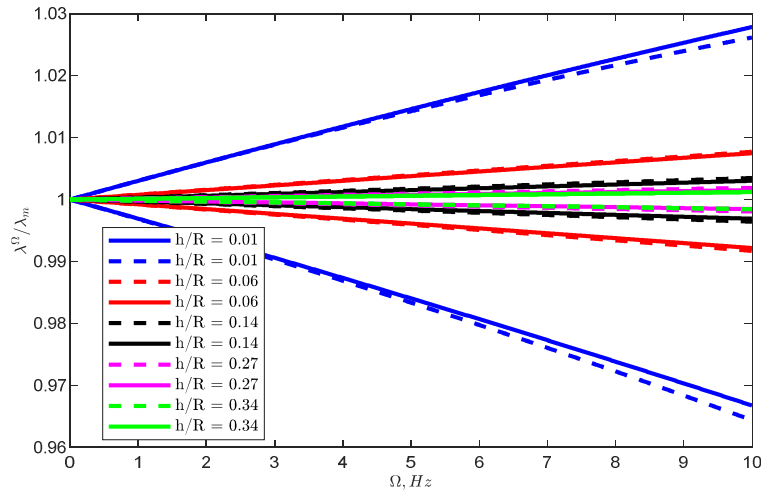
Fig. 10. The dependence of the natural frequency of the resonator in the case of forced circular motion on the angular velocity in the case of the Rayleigh solution (solid lines) and the solution when considering the potential energy of stretching (dashed lines) $(h/R = 0.01, 0.06, 0.14, 0.27, 0.34)$.
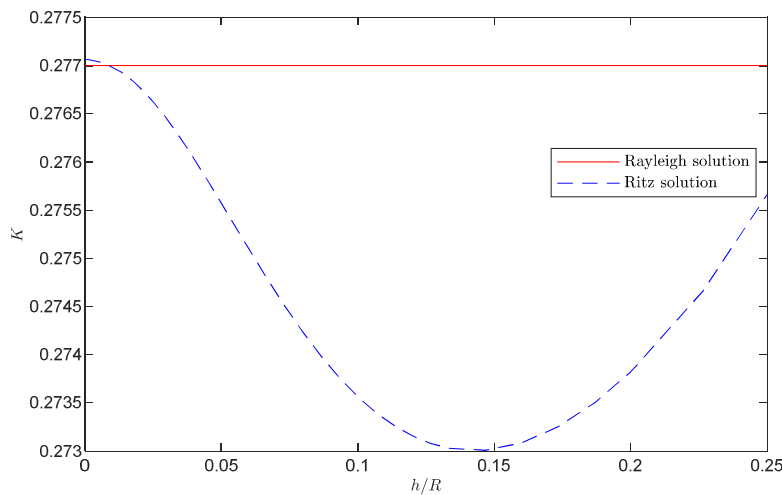

Fig. 11. Dependence of the precession coefficient K on the parameter h/R.

The solution of system (29) with regard to (30) with respect to the value of λ^Ω is written as:

$$\lambda^\Omega = \pm \frac{2\Omega I_3}{I_1} + \sqrt{\lambda_m^2 + \left(\frac{4I_3^2 - I_1 I_4}{I_1^2}\right)\Omega^2} \quad . \tag{31}$$

Equation (31) shows the dependence of natural frequencies of the resonator λ^Ω in the case of gyroscopic and centrifugal forces in forced circular motion of the resonator relative to its symmetry axis. The value of the splitting of natural frequencies λ_s^Ω according to (31) is written as:

$$\lambda_s^\Omega = \frac{4\Omega I_3}{I_1}. \tag{32}$$

Equation (32) shows that the value of λ_s^Ω depends linearly on the angular velocity of the external action Ω. For sufficiently small values $\Omega = [0.01\ 10]$ Hz the value of the splitting of the natural frequency is $\lambda_s^\Omega = [0.025\ 25]$ Hz, λ_m is in order kHz.

Figure 10 shows the dependences of the resonator's natural frequency λ^Ω on the angular velocity Ω at different values of h/R. This figure shows that the natural frequency λ^Ω of the resonator vibrations is almost linearly dependent on the frequency of external excitation for its typical operating range. Moreover, when considering the dependence of the eigenforms on the h/R parameter, it can be seen that the frequency spectrum shifts to the region of lower frequencies as compared to the case when classical Rayleigh functions are used.

Multiply the second equation (29) by i and add it to the first, introducing a complex function $z(t) = p(t) + iq(t)$ [27]:

$$\ddot{z} + \frac{4iI_3}{I_1}\Omega\dot{z} + \left(\lambda_m^2 - \frac{I_4}{I_1}\Omega^2\right)z = 0. \tag{33}$$

General solution of equation (33) can be written as:

$$z(t) = e^{-\frac{2iI_3}{I_1}\Omega t}\left(Z_1 e^{i\sqrt{\lambda_m^2 - \frac{I_4}{I_1}\Omega^2}t} + Z_2 e^{-i\sqrt{\lambda_m^2 - \frac{I_4}{I_1}\Omega^2}t}\right), \tag{34}$$

where Z_1, Z_2 are complex numbers determined by the initial conditions.

The expression (34) shows that the radius-vector of point z on the complex plane rotates with angular velocity $-2\Omega I_3/I_1$, in the direction opposite to the rotation of the resonator. This means that the standing wave changes orientation in the resonator body with angular velocity $\omega = -K\Omega$, where the Bryan coefficient K of the standing wave in the resonator is expressed by the equation [27, 28]:

$$K = \frac{2I_3}{I_1} = \frac{2\int_0^{\pi/2}[U(m,\theta)\cos\theta + W(m,\theta)\sin\theta]V(m,\theta)\sin\theta\,d\theta}{\int_0^{\pi/2}[U^2(m,\theta) + V^2(m,\theta) + W^2(m,\theta)]\sin\theta\,d\theta}. \tag{35}$$

Figure 11 shows a comparison of the standing wave precession coefficient in a hemispherical resonator on the parameter h/R. It shows that the precession coefficient of the hemispherical resonator, considering the dependence of the eigenforms on its thickness, has similar values compared to the use of classical Rayleigh forms. It is noted that the dependence of the Bryan coefficient is a non-monotone dependence in relation to the geometrical ratios of the resonator and it has a local minimum near the point $h/R = 0.14$. This fact allows us to state that designing a structure with such ratios will reduce the system sensitivity (its frequency splitting with parasitic precession) to geometrical imperfections [29].

7. Conclusion

Linear vibrations of a hemispherical RIG resonator were studied. It was shown that the analytical Rayleigh expressions for natural frequencies coincide with the experimental ones for small thicknesses of the resonator. Using the Ritz method, approximate dependences of the operating frequency and form of oscillations of the resonator on its thickness were obtained. It was shown that, when considering the potential energies of stretching and bending of the shell, the Ritz method delivers a more accurate fit for relatively thick shells. The application of the proposed approximate analytical approach makes it possible to estimate the vibration spectrum of the hemispherical resonator more accurately than the analytical expressions of Rayleigh, while remaining within the framework of the Kirchhoff-Love shell theory. The typical situations of the device operation, in which the frequency splitting effect is manifested, were considered. For these cases, it was shown that considering the dependence of the hemisphere eigenforms on the h/R ratio quantitatively changes the dependence of the frequency splitting magnitude both on the magnitude of the mass defect and on the magnitude of the angular velocity. Moreover, it was exhibited that the Bryan coefficient is considerably and non-monotonically dependent on the geometric parameters of the resonator. The model proposed in the paper allows one to analyze the effect of technologically determined imperfections and gyroscopic forces on the spectral characteristics of a hemispherical resonator with a significantly higher accuracy compared to the conventional Rayleigh approach, while maintaining the advantages of computational compactness.

Author Contributions

The manuscript was written through the contribution of all authors. All authors discussed the results, reviewed, and approved the final version of the manuscript.

Acknowledgments

Not Applicable.

Conflict of Interest

The authors declared no potential conflicts of interest concerning the research, authorship, and publication of this article.

Funding

Data Availability Statements

The datasets generated and/or analyzed during the current study are available from the corresponding author on reasonable request.

Nomenclature

h	Shell thickness [m]	u_m, v_m, w_m	Components of disp. vector in pure bending [m]
R	Radius of the median shell [m]	$\tilde{u}_m, \tilde{v}_m, \tilde{w}_m$	Components of disp. vector in bending/stretching [m]
E	Young's modulus [Pa]	U, V, W	Rayleigh eigenforms
ρ	Density [kg m^{-3}]	$\tilde{U}, \tilde{V}, \widetilde{W}$	Eigenforms obtained by the Ritz method
ν	Poisson's ratio	Π_b	Potential bending energy [J]
t	Time [s]	Π_s	Potential tensile energy [J]
$p(t), q(t)$	Modal coordinates [m]	$\Pi_f = \Pi_b + \Pi_s$	Total potential energy [J]
m	Number of oscillation form	T	Kinetic energy [J]

λ_m	The natural frequency of the resonator	$L = T_s - \Pi_b$	Lagrangian [J]
$\kappa_1, \kappa_2, \kappa_{12}$	Components of the bending strain tensor [m^{-1}]	δ	Physical value increment
e_1, e_2, e_{12}	Components of the tensile strain tensor [m^{-1}]	$C_i^U \ \ C_i^V \ \ C_{i-1}^W$	Ritz modal functions $(i = 3\ 5\ 7)$
θ, φ	Spherical coordinates [rad]	Ω_n	Vector of natural frequency
$A \ B$	Mass and stiffness matrices	Ω	Angular velocity [rad/s]
C	Vector of coordinate functions	T_s^ε	Kinetic energy in the case of imperfect resonator [J]
M	Number of own forms considered	T_s^Ω	Kinetic energy in the case of external angular velocity [J]
λ^Ω	Natural freq. in the case of external angular velocity [Hz]	λ	Natural frequency [Hz]
$\lambda_s^\Omega \ \ \lambda^\varepsilon$	The values of the splitting of natural frequencies [Hz]	K	Precession coefficient

References

[1] Matveev, V.A., Basarab, M.A., Lunin, B.S., Development of the theory of cylindrical vibratory gyroscopes with metallic resonators, *Vestnik RFBR,* 87(3), 2015, 84-96.

[2] Zhang, Y., Wu, Y., Wu, X., Xi, X., Wang, J., A novel vibration mode testing method for cylindrical resonators based on microphones, *Sensors,* 15(1), 2015, 1954-1963.

[3] Basarab, M.A., Lunin, B.S., Kolesnikov, A.V., Numerical-analytical solution of the differential equation of free oscillations of an elastic ring when an arbitrary law of rotation of the basement, *Dynamics of Complex Systems - XXI Century,* 2, 2020, 5-15.

[4] Matthews, A., Rybak, F.J., Comparison of hemispherical resonator gyro and optical gyros, *IEEE Aerospace and Electronic Systems Magazine,* 7(5), 1992, 40-46.

[5] Xu, Z., Yi, G., Qi, Z., Huang, C., Fang, H., Structural optimization research on hemispherical resonator gyro based on finite element analysis, *Chinese Control Conference,* Chengdu, China, 2016.

[6] Rozelle, D.M., The hemispherical resonator gyro: From wineglass to the planets, *AAS/AIAA Space Flight Mechanics Meeting,* Savannah, Georgia, 2009.

[7] Shatalov, M., Charlotta, C., Dynamics of rotating and vibrating thin hemispherical shell with mass and damping imperfections and parametrically driven by discrete electrodes, *Gyroscopy and Navigation,* 2(1), 2011, 27-33.

[8] Strutt, J.W., *The theory of sound,* Vol. 1, Macmillan, New York, 1877.

[9] Strutt, J.W., *The theory of sound,* Vol. 2, Macmillan, New York, 1896.

[10] Xu, Z., Yi, G., Qi, Z., Huang, C., Fang, H., Dynamic modeling and output error analysis of an imperfect hemispherical shell resonator, *Journal of Sound and Vibration,* 498, 2021, 115964.

[11] Nayfeh, A.H., *Perturbation methods,* John Wiley & Sons, New York, 2008.

[12] Goldenveizer, A.L., Theory of elastic thin shells, *Naval Engineering Journal,* 74(3), 1962, 582.

[13] Goldenveizer, A.L., Derivation of an approximate theory of shells by means of asymptotic integration of the equations of the theory of elasticity, *Journal of Applied Mechanics,* 27(4), 1963, 903-924.

[14] Love, E.H., *A treatise on the mathematical theory of elasticity,* Cambridge University Press, Cambridge, 2013.

[15] Budiansky, B., Notes on nonlinear shell theory, *Journal of Applied Mechanics,* 35(2), 1968, 393-401.

[16] Tuakalov, Y., Finite element model of Reisner's plate in stresses, *Magazine of Civil Engineering,* 89(5), 2019, 61-78.

[17] Greensplon, J.E., Vibrations of a Thick-Walled Cylindrical Shell—Comparison of the Exact Theory with Approximate Theories, *The Journal of the Acoustical Society of America,* 32(5), 1960, 571-578.

[18] Peng, Y.X., Zhang, A.M., Ming, F.R., A thick shell model based on reproducing kernel particle method and its application in geometrically nonlinear analysis, *Computational Mechanics,* 62(3), 2018, 309-321.

[19] Xu, Z., Xi, B., Yi, G., Ahn, C.K., High-precision control scheme for hemispherical resonator gyroscopes with application to aerospace navigation systems, *Aerospace Science and Technology,* 119, 2021 107168.

[20] Xu, Z., Zhu, W., Yi, G., Fan, W., Dynamic modeling and output error analysis of an imperfect hemispherical shell resonator, *Journal of Sound and Vibration,* 498, 2021,115964.

[21] Sorokin, S., Krylov, S., Darula, R., Reduced order modeling of vibration localization in a rotating toroidal shell for angular rate sensors applications, *Sensors and Actuators,* 332(2), 2021, 113054.

[22] Panovko, I.G., *Introduction to the theory of mechanical oscillations,* Moscow Izdatel Nauka, Moscow, 1980.

[23] Gilat, A., *MATLAB: An introduction with Applications,* John Wiley & Sons, New York, 2004.

[24] Thompson, M.K., Thompson, J.M., *ANSYS mechanical APDL for finite element analysis,* Butterworth-Heinemann, Oxford, 2017.

[25] Lin, Z., Fu, M., Deng, Z., Liu, N., Liu, H., Frequency Split Elimination Method for a Solid-State Vibratory Angular Rate Gyro with an Imperfect Axisymmetric-Shell Resonator, *Sensors,* 15(2), 2015, 3204-3223.

[26] Maslov, A.A., Maslov, D.A., Merkuryev, I.V., Podalkov, V.V., Compensation of wave solid gyroscope drifts caused by anisotropy of elastic properties of a monocrystalline resonator, *Gyroscopy and Navigation,* 28(2), 2020, 25-36. (In Russian)

[27] Matveev, V.A., Lipatnikov, V.I., Alechin, A.V., *Designing a wave solid gyroscope,* Bauman Moscow State Technical University, Moscow, 1997. (In Russian)

[28] Basarab, M.A., Kravchenko, V.F., Matveev, V.A., *Methods modeling and digital signal processing in gyroscopy,* Phizmatlit, Moscow, 2008. (In Russian)

[29] Merkuriev, I.V., Podalkov, V.V., *Dynamics of micromechanical and wave solid state gyroscope,* Phizmatlit, Moscow, 2009. (In Russian)

ORCID iD

D. Indeitsev https://orcid.org/0000-0001-9090-6970

P. Udalov https://orcid.org/0000-0002-9744-8869

I. Popov https://orcid.org/0000-0003-4425-9172

L. Alexei https://orcid.org/0000-0003-2016-8612

Publisher's Note Shahid Chamran University of Ahvaz remains neutral with regard to jurisdictional claims in published maps and institutional affiliations.